Contents lists available at GrowingScience

Decision Science Letters

homepage: www.GrowingScience.com/dsl

Multi-period supply chain optimization with contango and backwardation effects using an improved hybrid genetic algorithm

Mudassar Rauf [a*], Muhammad Imran[b], Jabir Mumtaz[a*], Saima Javed[c] and Ayesha Saeed[d]

[a]*Associate Professor, College of Mechanical and Electrical Engineering, Wenzhou University, Wenzhou, China*
[b]*Assistant Professor, Bang College of Business, KIMEP University Almaty, Kazakhstan*
[c]*Postgraduate, School of Management, Huazhong University of Science and Technology, Wuhan, China*
[d]*Postgraduate, School of transportation and logistics, Southwest Jiaotong University, China*

C H R O N I C L E

Article history:
Received: February 12, 2025
Received in revised format: March 12, 2025
Accepted: May 1 2025
Available online: May 2 2025

Keywords:
Multi-period supply chain
Contango-backwardation
Cost uncertainty modeling
Fuzzy regression
Improved hybrid genetic algorithm

A B S T R A C T

In real-world markets, supply chain costs often fluctuate over time due to the contango and backwardation effects, making multi-period supply chain planning complex and critical. This paper presents a multi-period supply chain optimization model that explicitly incorporates these effects into cost forecasting and decision-making. A multi-period supply chain model is developed, considering the cost uncertainty introduced by contango and backwardation. An integrated polynomial regression fuzzy method is proposed to address this problem by predicting future fluctuations in purchasing, ordering, and logistics costs. A mixed-integer linear programming (MILP) model is formulated to minimize the total supply chain cost across multiple periods. Moreover, improving the hybrid genetic algorithm (IHGA) is proposed to solve this problem. The performance of the proposed IHGA is triggered by integrating trust region, quasi-Newton, and pattern search methods. Response Surface Methodology (RSM) determines the optimal parameter settings and hybridization structure. A real-world case study involving surgical instrument manufacturing companies validates the proposed approach. The results highlight optimal supplier selection and order allocations for each period, and performance comparisons reveal that the IHGA outperforms traditional algorithms in terms of cost efficiency, computational time, and convergence behavior.

1. Introduction

Supply chains represent the structured flow of raw materials, products, services, and information across multiple entities. Effective supply chain management ensures product availability, timely delivery, and cost control. While various supply chains have been studied, ranging from agricultural produce to industrial components, the supply chain for life-saving products such as medicines, blood, and surgical instruments remains paramount. Within this domain, selecting appropriate suppliers is a strategic decision that significantly influences product quality. Specifically, procuring raw materials with the correct chemical composition directly impacts surgical outcomes in the surgical instrument industry. Therefore, supplier selection and raw material allocation must be handled with precision and foresight. Supply chain operations are inherently multi-period. The purchasing, ordering, and logistics costs vary over time due to technological changes, market fluctuations, evolving product trends, and quality requirements. Typically, long-term contracts between manufacturers and clients fix selling prices, even though actual production costs continue to change, often eroding profit margins. While many traditional models assume constant costs throughout all periods, this assumption

* Corresponding author.
E-mail address mudassarrauf16@gmail.com (M. Rauf) jabirmumtaz@live.com (J. Mumtaz)

ISSN 1929-5812 (Online) - ISSN 1929-5804 (Print)

doi: 10.5267/j.dsl.2025.5.001

rarely holds in real-world applications (Čuček et al., 2014; Zeballos et al., 2014). Instead, cost structures evolve due to uncertainty, necessitating dynamic and responsive supply chain strategies (Akbari & Karimi, 2015; Du et al., 2024).

Recent studies in multi-period supply chain modeling have primarily focused on uncertainty in demand, production, or capacity while overlooking cost-side uncertainties. For example, Vicente et al. (2025) and Soleimani et al. (2013) developed multi-period and multi-echelon models with fixed costs, limiting their ability to capture real-time financial variability. Similarly, approaches proposed by Pasandideh et al. (2015) and Özceylan and Paksoy (2013) focused on demand and capacity uncertainties using fuzzy environments but retained fixed cost structures. Although effective in constrained environments, these models fall short when applied to fluctuating markets where costs are neither stable nor predictable. The concepts of contango and backwardation offer a realistic representation of such uncertainty. In contango, the future cost of a commodity or service is higher than its current value, while in backwardation, future prices are lower than spot prices. These phenomena are commonly observed in fuel prices, raw material markets, and labor costs. For instance, procurement and quality inspection staff salaries follow a contango trend due to organizational increment policies. Conversely, the cost of certain raw materials, such as AISI 304 steel, fluctuates between contango and backwardation depending on external factors like international policies, environmental regulations, and supply disruptions.

Despite the practical importance of these cost fluctuations, they remain underexplored in the literature. Notably, Awudu and Zhang (2013) introduced cost uncertainty in biofuel supply chains, yet their model lacked the integration of price trend behaviors like contango and backwardation. Other works by Zeballos et al. (2014), Osmani and Zhang (2013), and Rodriguez et al. (2014) examined uncertainty in supply and demand, overlooking the dynamic nature of cost progression over time. Furthermore, models that consider future costs often assume strictly increasing or decreasing trends (Lalmazloumian et al., 2016; Marzband et al., 2015; Saffar & Razmi, 2015), which do not reflect the mixed nature of real-world pricing behavior. To address this gap, this study proposes a multi-period supply chain optimization model incorporating contango and backwardation effects into cost forecasting. An integrated polynomial regression fuzzy method is employed to model uncertain cost trends by combining historical regression-based predictions with fuzzy logic to capture deviations caused by unpredictable externalities. This dual-layer modeling ensures a more realistic forecast of ordering, purchasing, and transportation costs.

Numerous artificial intelligence techniques have been employed to solve complex supply chain network problems, particularly where traditional optimization methods fail to handle uncertainty and system complexity. Jamrus et al. (2015) integrated particle swarm optimization (PSO) and the GA to solve a supply chain network problem to minimize the overall supply chain costs. Mousavi et al. (2015) used a modified fruit fly algorithm to solve a location allocation-inventory control problem involving a distributer-retailer network. Fathian et al. (2018) used an improved electromagnetism-like algorithm to solve the problems of location-allocation and transportation planning in a supply chain. Garg (2016) used a hybridized GA and PSO to solve various constraint optimization problems. Changdar et al. (2015) improved the genetic algorithm (GA) by fine-tuning its parameters, including crossover and mutation. While GAs are widely applied in supply chain and logistics optimization (Afrouzy et al., 2016; Meena & Sarmah, 2013), their performance often deteriorates under constraint-heavy problems. To overcome this, the study develops an IHGA that integrates fine-tuning via response surface methodology (RSM) and hybridization with pattern search, quasi-Newton, and trust region methods. Prior research has treated tuning and hybridization independently, but this study demonstrates the benefit of combining both strategies to enhance cost, convergence speed, and computational efficiency. The proposed approach is validated through a real-world case study involving surgical instrument manufacturing firms. This research offers a novel contribution by integrating contango and backwardation effects into future cost prediction for a multi-period surgical supply chain, modeled using an integrated polynomial regression fuzzy method together with IHGA optimization methodology. The findings illustrate that modeling cost-side uncertainties with contango and backwardation effects yields more practical and flexible supply chain strategies, ultimately supporting better supplier decisions and resource allocations over time.

The remainder of this paper is organized as follows: Section 2 comprehensively describes the problem and the corresponding mathematical model. Section 3 presents a detailed explanation of the proposed IHGA. Section 4 discusses the computational experiments and analyzes the results obtained. Finally, Section 5 concludes the paper and outlines potential directions for future research.

2. Problem description and mathematical model

The first phase of this research focuses on developing the mathematical model. Each product and service within the selected supply chain is critically analyzed in this phase, and future cost trends are modeled considering uncertainty. An integrated polynomial regression fuzzy method is proposed to represent the uncertainty arising from contango and backwardation conditions. This modeling approach leads to a mixed-integer linear programming (MILP) model designed to minimize total supply chain costs across multiple time periods. The supply chain consists of a set of suppliers and manufacturers. Manufacturers procure raw materials from suppliers and convert them into final products. The supply of raw materials is not a one-time event but a recurring process that unfolds over multiple periods. A fundamental aspect of supply chain management is selecting the most suitable suppliers to fulfill demand efficiently. However, suppliers that perform well in one time period may not remain optimal in subsequent periods due to fluctuations in cost, delivery time, and product quality. Therefore, supplier selection must be reassessed periodically to ensure total supply chain costs are minimized across the planning horizon. Three scenarios are considered to capture the nature of cost fluctuations: contango, backwardation, and a mixed condition combining both.

Case 1- Contango: Contango describes a situation where future prices of products or services are higher than current (spot) prices. This condition is typically observed in scenarios involving predictable cost growth. For instance, ordering costs in a supply chain often follow a contango pattern because they are influenced by employee salaries, which generally increase over time. Therefore, future labor costs are higher than spot costs (Ribeiro & Hodges, 2005).

Case 2- Backwardation: Backwardation represents the inverse condition where future prices are lower than spot prices. This is often seen in technology products like computers or mobile phones, where innovation and competition drive prices downward over time (Miffre, 2000).

Case 3- Contango-backwardation: In practice, however, many cost elements do not follow a singular pattern. Instead, they exhibit mixed trends—commonly referred to as contango-backwardation—driven by complex external factors such as political decisions, environmental regulations, international trade laws, and market volatility. For example, logistics costs, which are highly sensitive to fuel prices, often follow this mixed pattern. Similarly, the price of AISI 304 steel, a key raw material in surgical instruments, fluctuates in response to multiple global influences, although with relatively lower volatility than fuel (Benth et al., 2008). Fig. 1 illustrates these three cost trends within a multi-period supply chain, i.e., contango, backwardation, and contango-backwardation.

Several assumptions are made to develop a realistic and practical model. The demand for raw materials in the current period is known, while future demand is forecasted. Oil price variations and steel price fluctuations are treated as uncertain variables across all time intervals. Manufacturers are assumed to have their transportation systems, and their purchasing budgets are known in advance for each period. Salary increments for employees occur at fixed rates, and both supplier capacities and the number of employees at each manufacturing facility remain constant over time. Hiring or firing during the planning horizon is not permitted. These assumptions enable the formulation of a structured yet flexible model that accommodates real-world uncertainties while aiming to minimize the total supply chain costs over multiple time periods.

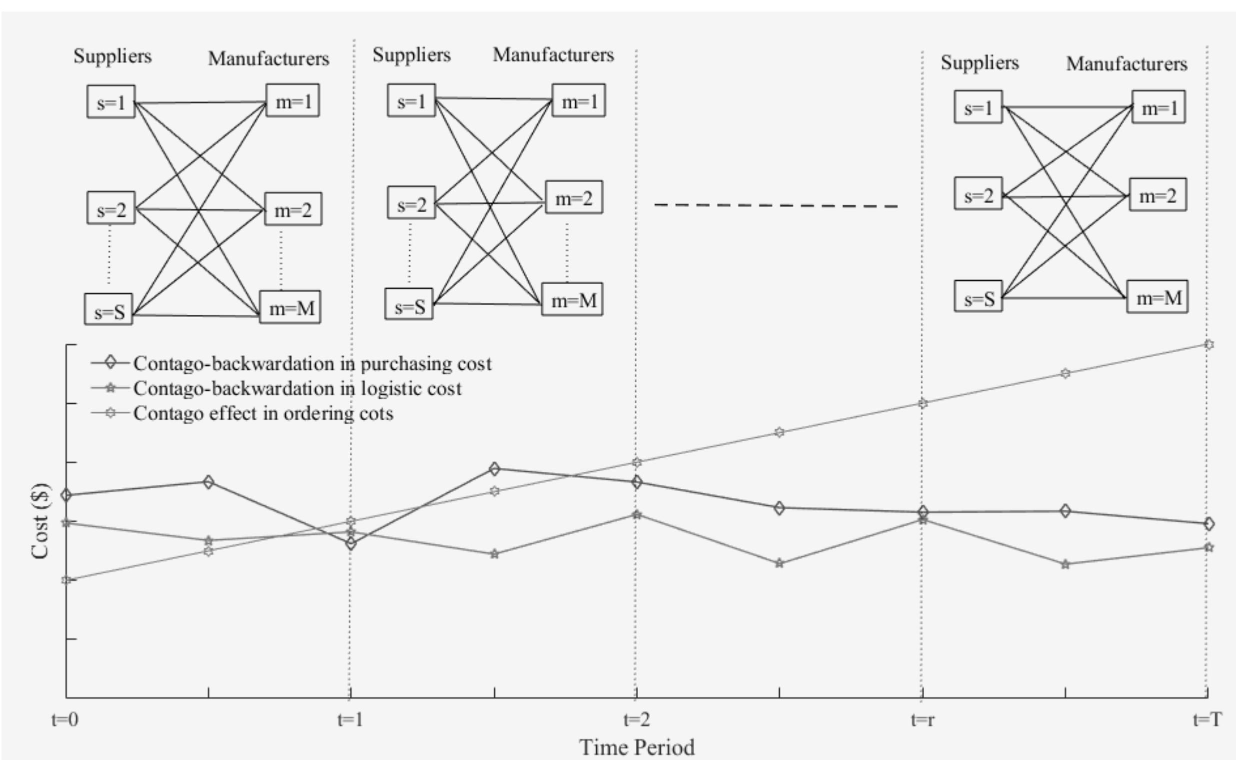

Fig. 1. Multi-period supply chain model with contango and backwardation effects

Table 1
Symbols and variables.

Notations	Meanings
p	Material part index
s	Supplier index
t	Time period index
m	Manufacturer index
i	Time interval index
j	Employee type index
k	Algorithm type index
r	Performance measure index
OC_{pmst}	Ordering cost of part material *"p"* in time period *"t"* by supplier *"m"* to supplier *"s"*
NO_{psmt}	Number of orders of part material *"p"* placed to supplier *"s"* by manufacturer *"m"* in time period *"t"*
W_{jmt}	The annual wage of employee type *"j"* of manufacturer *"m"* in time period *"t"*
L_{jmt}	Number of employees type *"j"* of manufacturer *"m"* in time period *"t"*
CPQ	Total cost of employees involved in purchasing and quality inspection
δ_{ij}^{w}	Change in salary of employee *"j"* in the interval *"i"*
PC_{pst}	Purchasing cost of part material *"p"* from supplier *"s"* in time period *"t"*
δ_{i}^{wp}	Change in purchasing price of part material in the interval *"i"*
δ_{i}^{o}	Change in oil price in interval *"i"*
α	Intercept of regression model
β	Slope of regression model
ε	Regression error
μ_x	Membership function of fuzzy variable *"x"*
A	Pessimistic value of triangular function
B	Optimistic value of triangular function
M	Most likely value of triangular function
τc	Transportation cost
OP_t	Oil price per liter in time period *"t"*
γ	Oil consumption rate
d_{sm}	Distance between supplier and manufacturer
V	Average speed of vehicle
D_{pmt}	Demand of part material *"p"* from manufacturer *"m"* in time period *"t"*
η_{pst}	Capacity of supplier *"s"* for part material *"p"* in time period *"t"*
AB_{mt}	Budget of manufacturer *"m"* in time period *"t"* for the purchase of raw material
MQ_{psmt}	Maximum order size that supplier *"s"* can supply to manufacturer *"m"* in time period *"t"*
AT_m	Maximum allowable delivery time by supplier to manufacturer
AR_p	Maximum allowable rejection rate
AV_{rk}	Achieved value of performance measure *"r"* of algorithm *"k"*
BV_r	Best value of performance measure *"r"* from set of *"K"* algorithms
G_{rk}	Gap between performance *"r"* of algorithm *"k"*

$$\mathrm{I}_{\mathrm{psmt}} = \begin{Bmatrix} 1 & \text{if supplier "}s\text{" provided material "}p\text{" to munufacutrer "}m\text{" in time period "}t\text{"} \\ 0 & \text{otherwise} \end{Bmatrix}$$

The total cost in the supplier selection and allocation problem comprises three major components: purchasing, logistics, and ordering costs. The ordering cost includes the salaries of purchase managers and marketing staff and the in-house quality inspection costs incurred when raw materials arrive at the manufacturer. Two types of employees are directly associated with ordering costs. The first type consists of executives involved in preparing purchase requisitions and orders and finance managers responsible for processing payments to suppliers. The second type comprises laborers assigned to inspect raw materials' quality upon arrival at the production facility. Since ordering costs depend on employee salaries, which are subject to periodic increments, these tend to rise over time. The ordering cost for each period can be calculated using the following equations.

$$Ordering\ cost\ =\ (Salary\ of\ employees\ involved\ in\ purchasing)\ +\ (in-house\ quality\ inspection\ cost) \tag{1}$$

$$OC_{pmst} = \left(\frac{Annualsalaryofemployee}{Numberofordersperanum} \times Totalnumberofemployess\right) \tag{2}$$

$$OC_{pmst} = \frac{1}{NO_{pmt}}\left(W_{jmt} \times L_{jmt}\right) \tag{3}$$

$$OC_{pmst} = \sum_{p=1}^{P}\sum_{s=1}^{S}\sum_{m=1}^{M}\sum_{t=1}^{T}\frac{1}{NO_{pmt}}\left(W_{jmt} \times L_{jmt}\right) \times I_{psmt} \tag{4}$$

Eq. (1) defines the total ordering cost. Eq. (2) calculates the per-unit ordering cost based on annual salary and the number of orders. Eq. (3) expresses this cost in terms of wage and labor variables, and Eq. (4) represents the aggregated ordering cost across all part types, suppliers, manufacturers, and time periods.

2.1 Contango effects on ordering costs

In traditional multi-period models, cost is assumed to be fixed in all periods. In reality, however, labor costs are not the same across time because salary incremental policies in each organization ensure that organizations maintain their current workforce. A contango situation occurs when the spot price of labor is lower than the future price of labor [24]. If we consider the salary incremental policy of organizations, then labor costs follow contango effects. If "δ_y^w" is the percentage of salary increment in time period "*t*", then adding this policy in Equation (4) yields Equation (5). Equation (5) is valid when the salary increment remains constant in all time periods for all types of employees. Finally, we get Equation (6), which is the ordering cost considering the contango effect.

$$OC_{pst} = \sum_{p=1}^{P}\sum_{j=1}^{J}\sum_{m=1}^{M}\sum_{t=1}^{T}\sum_{j=1}^{J}\frac{1}{NO_{psmt}}\left(W_{jmt} \times L_{jmt}\right) \times (1+\delta_{ij}^{w})^{t} \tag{5}$$

$$OC_{pst} = \sum_{p=1}^{P}\sum_{j=1}^{J}\sum_{m=1}^{M}\sum_{t=1}^{T}\sum_{j=1}^{J}\frac{1}{NO_{pmt}}\left(W_{jmt} \times L_{jmt}\right) \times (1+\delta_{ij}^{w})^{t} \times I_{psmt} \tag{6}$$

2.2 Contango and backwardation in purchasing costs

Contango and backwardation are opposite phenomena to one another. In a backwardation situation, the future prices of products or processes are less than the spot price. Various commodities and processes are subject to either contango or backwardation phenomena. In a surgical supply chain, the price of steel follows a mixed situation of contango and backwardation because there are many determinants of steel prices, including changes in technology, market competition, alternative materials, and organizational policies. Therefore, modeling the price of steel under only one contango or backwardation would not be feasible. However, the price of steel can be modeled using both situations. Past prices across the previous few years must be known to predict future prices. Here, we propose an integrated polynomial regression fuzzy model for predicting future prices in contango-backwardation situations. This method consists of the following steps. Let "δ " be the price difference between two consecutive periods. In other words, it is the difference in price in an interval of two successive time periods.

$$\delta_i^p = \begin{bmatrix} PC_{pst} - PC_{ps(t-1)} = \delta_1^p \\ PC_{pst(t-1)} - PC_{ps(t-2)} = \delta_2^p \\ PC_{pst(t-2)} - PC_{ps(t-3)} = \delta_3^p \\ . \\ . \\ PC_{ps(t-(n-1))} - PC_{ps(t-n)} = \delta_n^p \end{bmatrix} \tag{7}$$

As there are “n” past intervals, so we get a matrix of size “$n \times 1$”, which is shown in Eq. (7). By using the values of “δ_i^p”, we can establish a polynomial regression model with parameter “β ” and error “ε ” as shown in Eq. (8). To formulate the future purchasing cost formula, we can write the following relationship between spot and future prices.

$$\delta_{i+1}^p = \beta_0 + \beta_1 \times t_{i+1}^2 + \beta_1 \times t_{i+1}^3 \ldots\ldots\ldots + \beta_1 \times t_{i+1}^k + \varepsilon \tag{8}$$

$$PC_{pst} = PC_{ps1} \times \prod_{t=1}^{T}\left(1 + \delta_{i+1}^p\right) \qquad t = 2,3,\ldots,T \tag{9}$$

Eq. (9) shows the predicted future purchasing price of part material “p” at time period “t”, but it does not consider uncertainty in price changes. Price changes are uncertain because of the involvement of various factors, such as government policies, market competitiveness, the environment, and other unknowable factors. Any price change must be treated as a fuzzy variable to model this uncertainty. The fuzzification process consists of the following steps.

2.2.1 Determination of the membership function

Determination of the membership function is the first step in the fuzzification process. The membership function shows the shape of the curve within which the value of an uncertain variable lies. The most commonly used membership functions are triangular and trapezoidal, but their use depends on the nature of the data. In this problem, we have analyzed past material data for parts (AISI 204 stainless steel), finding that it follows the triangular membership function. Equation (10) shows the triangular membership function. Figure 1 is the graphical representation of a membership function in which “a, b and m” are the parameters of the membership function. Because “ δ_{i+1}^p ” is the fuzzy variable, $a = \delta_{i+1}^p - \Delta_1$, $m = \delta_{i+1}^p$, and $b = \delta_{i+1}^p + \Delta_2$. Inserting values of “a, b and m” in Eq. (10), we obtain the final membership function for uncertain changes in price as shown in Eq. (11).

$$\mu_x = \begin{Bmatrix} \frac{x-a}{m-a} & a \le x \le m \\ \frac{b-x}{b-m} & m \le x \le b \\ 0 & otherwise \end{Bmatrix} \tag{10}$$

$$\mu_{x(\delta_{i+1}^p)} = \begin{Bmatrix} \frac{x-\delta_{i+1}^p+\Delta_1)}{\Delta_1} & \delta_{i+1}^p - \Delta_1 \le x_{(i+1)} \le \delta_{i+1}^p \\ \frac{\delta_{i+1}^p+\Delta_2-x}{\Delta_2} & \delta_{i+1}^p \le x_{(i+1)} \le \delta_{i+1}^p - \Delta_2 \\ 0 & otherwise \end{Bmatrix} \tag{11}$$

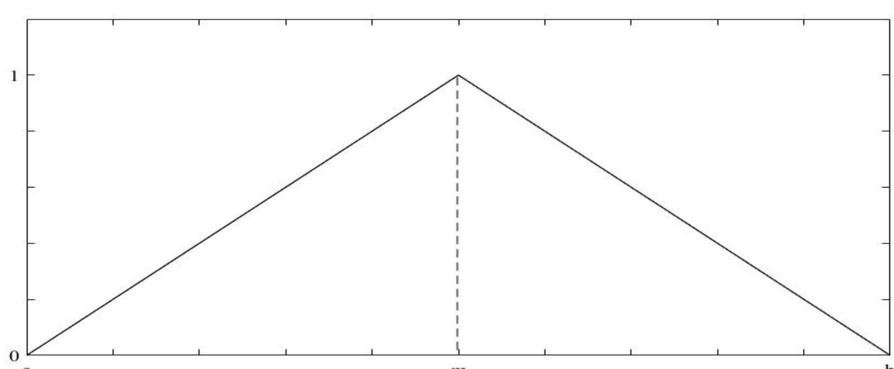

Fig. 1. Triangular membership function

2.2.2 Fuzzification

In consideration of "$PC_{pst} = y$" and "$\delta^p = x$", Eq. (11) changes to Eq. (12). If we consider *"t=1"*, then Eq. (12) reduces to Eq. (13). By solving Eq. (13) for the value of *"$x_{(i+1)}$"*, we get Eq. (14). Putting the value of *"$x_{(i+1)}$"* from Eq. (14) to the limits of Equ. (11), we get Eqs. (15-16). We get Eqs. (15-16) from Eqs. (17-19).

$$y = PC_{ps1} \times \prod_{t=1}^{T}(1 + x_{(i+1)}) \qquad t = 2,3,\ldots,T \tag{12}$$

$$y = PC_{ps1} \times \left(1 + x_{(i+1)}\right) \qquad t = 2,3,\ldots,T \tag{13}$$

$$x_{(i+1)} = \frac{y - PC_{pst}}{PC_{ps1}} \tag{14}$$

$$(\delta_{i+1}^{p} - \varDelta_1) \times PC_{ps1} + PC_{pst} \leq y \leq \delta_{i+1}^{p} \times PC_{ps1} + PC_{pst} \tag{15}$$

$$\delta_{i+1}^{p} \times PC_{ps1} + PC_{pst} \leq y \leq (\delta_{i+1}^{p} + \varDelta_2) \times PC_{ps1} + PC_{pst} \tag{16}$$

$$y_1 = (\delta_{i+1}^{p} - \varDelta_1) \times PC_{ps1} + PC_{pst} \tag{17}$$

$$y_2 = \delta_{i+1}^{p} \times PC_{ps1} + PC_{pst} \tag{18}$$

$$y_3 = (\delta_{i+1}^{p} + \varDelta_2) \times PC_{ps1} + PC_{pst} \tag{19}$$

2.2.3 Defuzzification

Defuzzification converts a fuzzified model to a crisp model. There are many methods for defuzzification, but the centroid method is extensively utilized because it is easy to use. Eq. (20) shows the center of gravity formula. Using Equations (17-20), we compute the final crisp model following defuzzification as given in Eq. (21) and Eq. (22). If we consider time period "T", then this becomes Eq. (23), as follows,

$$y = \frac{\sum_{j=1}^{J} y_j}{J} \tag{20}$$

$$y = PC_{ps1} \times \left((\delta_{i+1}^{p} + 1) + \frac{(\varDelta_2 - \varDelta_1)}{3}\right) \tag{21}$$

$$PC_{pst} = PC_{ps1} \times \left((\delta_{i+1}^{p} + 1) + \frac{(\varDelta_2 - \varDelta_1)}{3}\right) \tag{22}$$

$$PC_{pst} = PC_{ps1} \times \prod_{t=1}^{T}\left((\delta_{i+1}^{p} + 1) + \frac{(\varDelta_2^{p} - \varDelta_1^{p})}{3}\right) \tag{23}$$

2.3 Transportation costs with contango-backwardation effects

The costs of transportation depend mainly on the price of fuel. Changes in oil prices also follow contango-backwardation effects, as oil prices fluctuate significantly due to global market competition, political, and geographical factors. Eq. (24) shows the relationship between the spot price and the future price of fuel oil. As changes in oil prices are uncertain, oil prices are also treated as a fuzzy variable. The triangular membership function is found based on past oil price data. The same processes of fuzzification and defuzzification are repeated for Eq. (24). Finally, we get Eq. (25). Eq. (26) is the transportation cost function. Inserting the value of "OC_{pst}" in Equation (26), we get Eq. (27). The final function of the purchasing cost is represented in Eq. (28). By combining Eq. (26) and Eqs. (27-28), we get the final total cost function as given in Eq. (29).

$$OP_{pst} = OP_{ps1}\left(\prod_{t=1}^{T}(1 + \delta_{i+1}^{o})\right) \tag{24}$$

$$OP_{pst} = OP_{ps1} \times \prod_{t=1}^{T}\left((\delta_{i+1}^{p} + 1) + \frac{(\varDelta_2^{o} - \varDelta_1^{o})}{3}\right) \tag{25}$$

$$\tau c = \sum_{p=1}^{P}\sum_{s=1}^{S}\sum_{m=1}^{M}\sum_{t=1}^{T} OC_{pst} \times \gamma \times d_{sm} \tag{26}$$

$$\tau c = \sum_{p=1}^{P}\sum_{s=1}^{S}\sum_{m=1}^{M}\sum_{t=1}^{T}\left\{\gamma \times d_{sm} \times OC_{ps1} \times \prod_{t=1}^{T}\left((\delta_{i+1}^{p} + 1) + \frac{(\varDelta_2^{o} - \varDelta_1^{o})}{3}\right)\right\} \times I_{psmt} \tag{27}$$

$$\rho c = \sum_{p=1}^{P}\sum_{s=1}^{S}\sum_{m=1}^{M}\sum_{t=1}^{T} PC_{ps1} \times \prod_{t=1}^{T}\left((\delta_{i+1}^{p}+1)+\frac{(\Delta_2^p-\Delta_1^p)}{3}\right) \times Q_{pmst} \tag{28}$$

$$TC = \sum_{p=1}^{P}\sum_{s=1}^{S}\sum_{m=1}^{M}\sum_{t=1}^{T}\left\{\frac{1}{NO_{ps}} \times \{(W_e \times L_E)+(W_o \times L_O)\} \times (1+\Delta_t)^t\right\} \times I_{psmt}$$
$$+\sum_{p=1}^{P}\sum_{s=1}^{S}\sum_{m=1}^{M}\sum_{t=1}^{T}\left\{\gamma \times d_{sm} \times OC_{ps1} \times \prod_{t=1}^{T}\left((\delta_{i+1}^{p}+1)+\frac{(\Delta_2^o-\Delta_1^o)}{3}\right)\right\} \times I_{psmt} \tag{29}$$

$\sum_{p=1}^{P}\sum_{s=1}^{S}\sum_{m=1}^{M}\sum_{t=1}^{T}\left\{PC_{ps1} \times \prod_{t=1}^{T}\left((\delta_{i+1}^{p}+1)+\frac{(\Delta_2^p-\Delta_1^p)}{3}\right)\right\} \times Q_{pmst}$

2.4 Constraints

$$\sum_{s=1}^{S} Q_{psmt} = D_{pmt} \forall_p; \forall_m; \forall_t \tag{30}$$

$$\sum_{m=1}^{M} Q_{pmst} \leq (\eta_{pst} \times I_{pmst}) \forall_p; \forall_s; \forall_t \tag{31}$$

$$\sum_{p=1}^{P}\sum_{s=1}^{S}\sum_{m=1}^{M}\left\{PC_{ps1} \times \prod_{t=1}^{T}\left((\delta_{i+1}^{p}+1)+\frac{(\Delta_2^p-\Delta_1^p)}{3}\right)\right\} \times Q_{psmt} \leq AB_t \forall_t \tag{32}$$

$$Q_{psmt} \leq MQ_{psmt} \times I_{pmst} \forall_p; \forall_s; \forall_m; \forall_t \tag{33}$$

$$\frac{d_{ms}}{v} \times I_{psmt} \leq AT \forall_p; \forall_s; \forall_m; \forall_t \tag{34}$$

$$r_{psmt} \times I_{psmt} \leq AR_p \forall_p; \forall_s; \forall_m; \forall_t \tag{35}$$

$$Q_{psmt} \geq 0 \forall_p; \forall_s; \forall_m; \forall_t \tag{36}$$

$$I_{psmt} \in \{0,1\} \forall_p; \forall_s; \forall_m; \forall_t \tag{37}$$

Eq. (25) is the objective function of the total cost, which is composed of ordering, purchasing, and transportation costs with contango and backwardation effects. Eq. (26) shows the demand constraint, with demand being generated from the manufacturer. The constraint in Eq. (27) represents the capacity of each supplier to supply parts to the manufacturer. In contango and backwardation situations, fluctuations in budget increase dramatically. Accordingly, we have introduced a budget constraint in Eq. (28), which restricts costs in the budget. Eq. (29) shows the maximum order a supplier can supply to a manufacturer in time period “t”. Logistic time constraints are represented in Eq. (30). A defect rate measures steel quality; accordingly, Eq. (31) ensures that the defect rate is less than the acceptable limit. Eq. (32) is a non-negativity constraint, and Eq. (33) shows the binary variable.

3. Proposed metaheuristic approach

A genetic algorithm (GA) is an evolutionary computation method widely used to solve complex optimization problems. Darwinian natural selection principles inspire it and operate on a population of individuals, where each individual represents a feasible solution. Through genetic operations—such as selection, crossover, and mutation—a new generation is produced iteratively until the optimal or near-optimal solution is achieved. The GA has been extensively applied in supply chain optimization problems (Afrouzy et al., 2016; Meena & Sarmah, 2013; Soleimani et al., 2013). However, its performance degrades when applied to constrained problems, especially equality constraints. Prior studies have improved GA performance by fine-tuning its parameters or hybridizing it with other algorithms to address this. However, these studies explored only one improvement avenue: fine-tuning or hybridization. In contrast, the proposed methodology introduces a combined enhancement approach: simultaneous fine-tuning and hybridization, thereby capturing both benefits.

In this methodology, we first identify the GA parameters with the most significant influence on performance: population size and crossover rate. A small population size may reduce computational time but compromise the quality of solutions. Besides, a large population size increases computational time with a higher likelihood of convergence to optimal solutions. Similarly, a high crossover rate enhances population diversity, reduces the required generations, and increases computational overhead. Likewise, hybridizing GA with local search algorithms improves solution quality but adds to computational cost. Therefore, an optimal balance among these parameters is crucial. To achieve this balance, we employ RSM. The input factors in RSM include population size, crossover rate (both continuous), and the choice of hybrid function (categorical). The output responses measured are total cost, computational time, and the number of generations/iterations required for convergence.

The steps involved in our proposed methodology are as follows. First, we identify the GA parameters that significantly influence performance regarding objective function value, computational time, and the number of generations. This study selects population size and crossover rate as the most impactful parameters. Next, we determine which algorithms are suitable candidates for hybridization with GA. For this purpose, pattern search, trust region, and quasi-Newton methods are chosen. These hybrid functions are treated as a categorical factor with three defined levels. In contrast, population size and crossover rate are considered continuous variables. A central composite design (CCD) under the response surface methodology (RSM) framework is employed to structure the experimental setup for parameter tuning. The GA is then executed for each experimental run, and corresponding responses, namely, total cost and computational time are recorded. Using the collected data, response surfaces are generated to model the relationships between the input parameters and performance outcomes. These surfaces extract optimal values of the crossover rate, population size, and the most effective hybrid function. The GA is then hybridized using the best-performing function, and the optimal parameter values are applied. If termination criteria are met, the process is terminated. Otherwise, the tuning cycle is repeated, starting from the experimental design phase. The step-by-step procedure for the implementation of the proposed IHGA is given below.

Algorithm: Steps of proposed IHGA

```
Begin IHGA
// Step 1: Identify GA Parameters
Define key parameters: population size, crossover rate
Select candidate hybrid functions: (Pattern Search, Trust Region, Quasi-Newton)
// Step 2: Parameter Classification
Classify:
   - Population size and crossover rate → Continuous
   - Hybrid function → Categorical
// Step 3: Experiment Design via RSM
Use Central Composite Design (CCD) to structure experimental runs
For each parameter combination:
   Run GA with selected hybrid function
   Record performance: cost and computational time
// Step 4: Analyze Results
Construct response surfaces
Identify optimal values of population size, crossover rate, and best hybrid function
// Step 5: Execute Optimized GA (IHGA)
Initialize population with optimal population size
While termination criteria not met:
   Select parents
   Apply crossover (with optimal rate)
   Apply mutation
   Evaluate offspring
   Select individuals for next generation
Apply the best hybrid function for local refinement
// Step 6: Evaluate IHGA Performance
If termination criteria is met:
   Terminate
Else:
   Return to Step 3 and repeat tuning
End IHGA
```

3.1 Example case problem

A real-world case study involving a group of surgical companies is presented to solve the formulated mathematical model using the proposed approach. These companies are based in Sialkot, Pakistan, and operate three manufacturing plants that produce surgical instruments, including knife handles, scissors, forceps and clamps, retractors, suction tubes, orthopedic instruments, and cardiac, vascular, and thoracic instruments. The manufacturing processes rely on various grades of stainless steel (AISI 302–AISI 316), depending on the specific product type. In particular, AISI 304 steel is used to produce scissors, representing the highest volume of orders the group receives. The companies manage their logistics and use in-house transportation to collect raw materials from suppliers. The average fuel consumption is 0.0385 liters per kilometer, with an average vehicle speed of 70 kilometers per hour. Company executives, including the CEO, have expressed concern about the uncertain fluctuations in AISI 304 steel and diesel oil prices over time. These price changes significantly impact profitability, especially since customers often establish long-term price agreements. As production costs rise—driven by variability in raw material and fuel prices—the profit margin narrows, making it increasingly difficult to maintain financial stability. The group recognizes the need for strategic supply chain planning over multiple periods, specifically over a five-year horizon. This planning must incorporate certain and uncertain elements: certain increases in ordering costs due to employee salary increments and uncertain variations in purchasing and transportation costs driven by external market dynamics.

The plan is constrained by a fixed budget of $30,000,000, a maximum delivery time of six hours, and an acceptable quality threshold defined by a maximum rejection rate of 3%. The annual forecasted demand for AISI 304 steel for each manufacturer over the planning horizon is presented in Table 2. Six suppliers supply AISI 304 steel to the manufacturing plants. Distances between suppliers and manufacturers are given in Table 3. The expected number of orders placed by manufacturers for AISI 304 steel is shown in Table 4. Purchasing cost is the cost of AISI 304 steel. Table 6 shows the cost of AISI 304 steel per kilogram from each supplier in the current time period.

Table 2
Annual forecasted demand of AISI 304 steel (kg) from each manufacturer in each time period

Time/ Manuf.	*t=1*	*t=2*	*t=3*	*t=4*	*t=5*
m=1	8,500	4,000	3,250	3,080	3,100
m=2	3,300	3,700	4,050	4,050	3,200
m=3	4,800	4,350	4,000	4,400	4,800

Table 3
Distances between suppliers and manufacturers in kilometers

Supplier/Manuf.	*s=1*	*s=2*	*s=3*	*s=4*	*s=5*	*s=6*
m=1	120	134	87	63	102	76
m=2	95	57	173	154	134	44
m=3	72	162	127	84	87	83

Table 4
Expected number of orders placed by manufacturers in each period

Manuf./Time	*t=1*	*t=2*	*t=3*	*t=4*	*t=5*	*t=6*
m=1	203	207	211	212	217	219
m=2	176	181	182	191	193	196
m=3	234	121	231	125	213	123

Table 5
Total no. and annual salary of each employee type in period t=0 and salary increment per year

Manuf.	*m=1*		*m=2*		*m=3*	
Employer	*j=1*	*j=2*	*j=1*	*j=2*	*j=1*	*j=2*
L_{jmt}	22	65	15	78	141	204
W_{jmt} ($)	8,400	3,600	9,000	4,000	9,300	3,750
δ_{ij}^{w}	18 %	18%	17%	17 %	15 %	15 %

Table 6
Purchasing cost ($) of AISI 304 steel per kilogram from each supplier

Cost	*s=1*	*s=2*	*s=3*	*s=4*	*s=5*	*s=6*
PC_{ps1}	2.20	2.65	1.65	1.98	2.20	2.31

It is clear from Fig. 3 that fluctuations in the price of AISI 304 steel across the last five years follow contango and backwardation effects. Changes in steel prices are uncertain, so the variable is considered fuzzy. Based on data from the past five years, changes in the price of AISI 304 steel are modeled in polynomial regression. Programming language MATLAB R2017a is used to find a regression model for future changes in steel price prediction. Eq. (38) shows the relationship between future price changes and current time periods. The adjusted R-squared value for this model is 0.68, the sum of squared errors is 0.18, R-squared is 0.7114, and the root-mean-square error is 0.05524. If we use forecasted data only, the curve fitting will follow only increasing or decreasing trends. However, fluctuations in price changes are uncertain, and therefore, changes in future prices are uncertain or fuzzy. Table 6 shows the values of deviational variables for each period. These deviational variables predict uncertain changes in the AISI 304 steel prices over time. A set of expert and past data analysis have decided the values of these variables. Using Equation (38), Equation (28), and Table 6, we can compute the future purchasing costs of AISI 304 steel. Similarly, transportation costs are a function of diesel oil prices. Changes in oil prices are in a contango-backwardation situation, so we followed the same procedure to predict changes in future time periods. Figure 3 shows the curve fitting of data for diesel oil prices across the last five years. Equation (39) represents the polynomial regression for changes in oil prices.

$$\delta_{i+1}^{p} = -2.88 \times 10^{-8} \times t^5 + 4.88 \times 10^{-6} \times t^4 - 2.92 \times 10^{-4} \times t^3 + 7.282 \times 10^{-3} \times t^2 - 6.63 \times 10^{-2} \times t + 0.1293 \tag{38}$$

$$\delta_{i+1}^{o} = -1.88 \times 10^{-7} \times t^4 + 2.27 \times 10^{-5} \times t^3 - 0.00086 \times t^2 + 0.01057 \times t - 0.02926 \tag{39}$$

The adjusted R-squared value for Eq. (39) is 0.772, the sum of squared errors is 0.05126, the value of R-squared is 0.7872, and the root-mean-square error (RMSE) is 0.03025. Table 8 shows the deviational variables for changes in the change of oil prices across time. Experts and past data have decided the values of these variables.

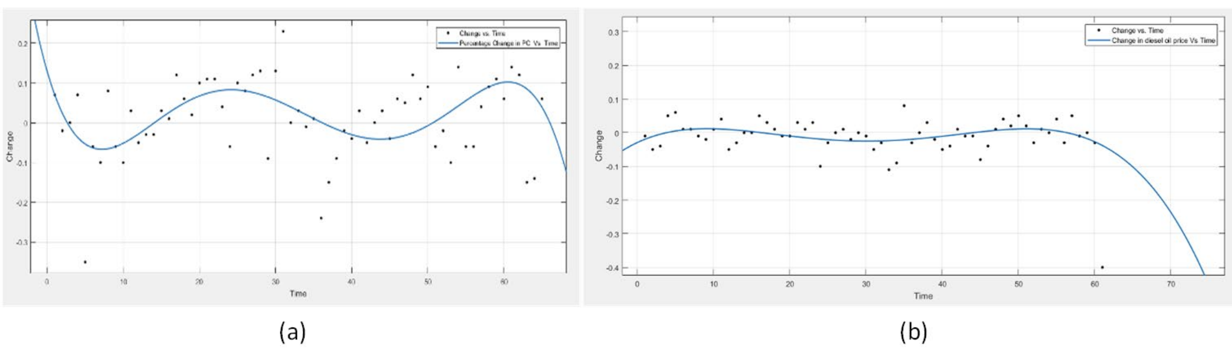

Fig. 2. Curve fitting of the last five years' prices of (a) AISI 304 steel and (b) diesel oil

Table 7
Deviational variables for changes in the change of future purchasing price of AISI 304 steel

Price changes	t=1	t=2	t=3	t=4	t=5	t=6
Δ_1^p	-0.03	-0.33	-0.27	0.10	-0.23	-0.37
Δ_1^p	0.20	-0.11	0.16	0.31	0.245	0.26
Δ_1^o	-0.05	-0.05	-0.11	-0.08	-0.03	-0.05
Δ_2^o	-0.01	0.05	0.05	0.08	0.05	-0.01

Logistic costs can be computed using Eq. (27). There are six suppliers, and each supplier's capacity is known and remains the same for all periods. Table 8 shows the capacity of each supplier.

Table 8
Capacity of each supplier to supply AISI 304 steel in kilograms

Capacity	*s=1*	*s=2*	*s=3*	*s=4*	*s=5*	*s=6*
η_{ps}	9,000	8,000	7,950	8,000	9,000	8,500

Because the suppliers deal with many other manufacturers, they provide maximum order quantities to a given manufacturer in a certain period of time. The maximum order quantity that a supplier can supply to a manufacturer is presented in Table 9.

Table 9
Maximum order quantity that a supplier can supply to a manufacturer

Order quantity	*s=1*	*s=2*	*s=3*	*s=4*	*s=5*	*s=6*
MQ_{psmt}	4,500	3,000	2,500	4,000	3,500	2,700

The group of companies wants to decide the quantity of steel and which supplier will supply AISI steel to which manufacturer in time period “t”.

3.2 Implementation of proposed methodology

The proposed IHGA is employed to solve this model. The chromosome structure designed for this problem is three-dimensional, comprising 180 genes. Among these, 90 genes are continuous variables, while 90 are binary. Due to the high dimensionality of the chromosome, only the structure corresponding to a single period is presented for illustrative purposes in Table 10.

Table 10
Chromosome structure for period “*t=1*”

	t=1					
Manuf.	*s=1*	*s=2*	*s=3*	*s=4*	*s=5*	*s=6*
m=1	3,500	200	200	200	200	200
m=2	2,000	660	660	660	660	660
m=3	3,800	0	0	0	0	0
m=1	1	1	1	1	1	1
m=2	1	1	1	1	1	1
m=3	1	0	0	0	0	0

As explained above, GA performance depends on the values of specific parameters, such as population size, crossover rate, mutation rate, and generation gaps. However, the values of crossover rate and population have more impact on performance than other operators, such as mutation rate and generation gaps. The first step in determining the optimal parameters for the improved hybrid GA (IHGA) involves defining the relevant factors and their corresponding levels. Three key factors are considered in the experimental design. The first is a categorical factor—algorithm type—which includes three levels: pattern search, trust region, and quasi-Newton. The second factor is the crossover rate, evaluated at three levels: 0.4, 0.6, and 0.8. The third factor is population size, which is tested at 50, 100, and 150. In the second step, a central composite design (CCD) is employed to model the experimental setup using response surface methodology. Each experiment is executed in MATLAB (R2017a) on a machine equipped with 8 GB RAM and a 3.40 GHz processor. Three performance metrics—cost, computational time, and number of generations—are recorded for each experimental run. The complete experimental design and the corresponding results are presented in Table 11. The data collected from Table 11 is then used to construct a response surface that identifies the optimal parameter configuration for the IHGA. Figure 4 illustrates the response surface, showing how performance varies with changes in parameter levels. From the analysis, it is evident that hybridizing the GA with the pattern search function, using a crossover rate of 0.56671 and a population size of 100, yields superior cost minimization, computational efficiency, and faster convergence results. The findings from Fig. 4 confirm that the IHGA, when fine-tuned and hybridized with pattern search, provides significantly improved performance compared to other configurations.

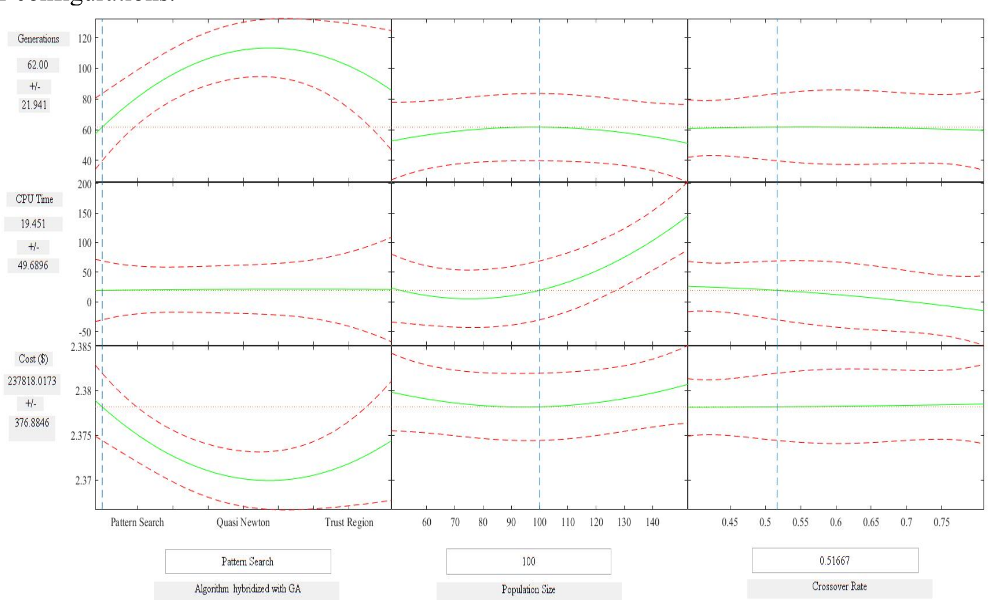

Fig. 3. Response surface

Table 11
Central composite design (CCD) of experiment and corresponding responses

Exp.	Real factors			Responses		
	Hybrid function	Population size	Crossover rate	Cost	Computational time	Generations
1	Pattern search	50	0.4	238059.22	11.12	50
2	Pattern search	50	0.8	238059.22	6.11	50
3	Pattern search	150	0.4	238059.22	171.10	42
4	Pattern search	150	0.8	238059.22	72.27	51
5	Trust region	50	0.4	237200.38	12.15	99
6	Trust region	50	0.8	237200.38	7.04	99
7	Trust region	150	0.4	237396.00	180.61	99
8	Trust region	150	0.8	237311.70	73.64	99
9	Pattern search	100	0.6	238059.22	16.78	51
10	Trust region	100	0.6	237200.40	17.74	99
11	Quasi-Newton	50	0.6	237200.40	9.52	99
12	Quasi-Newton	150	0.6	237306.10	126.83	99
13	Quasi-Newton	100	0.4	237200.40	22.37	99
14	Quasi-Newton	100	0.8	237200.40	13.41	99
15	Quasi-Newton	100	0.4	237200.40	22.20	99
16	Quasi-Newton	100	0.4	237200.40	22.41	99
17	Quasi-Newton	100	0.4	237200.38	21.85	99
18	Quasi-Newton	100	0.4	237200.38	21.02	99
19	Quasi-Newton	100	0.4	237200.40	23.43	99
20	Quasi-Newton	100	0.4	237200.40	22.66	99
21	Quasi-Newton	100	0.4	237200.38	27.63	99
22	Quasi-Newton	100	0.4	237200.40	26.99	99
23	Quasi-Newton	100	0.4	237200.40	29.32	99
24	Quasi-Newton	100	0.4	237200.40	28.89	99

4. Analysis of Results

The mixed-integer linear programming (MILP) model developed for this study consists of 180 decision variables, 301 inequality constraints, and 15 equality constraints. The optimal solution was obtained in 51 generations, resulting in a minimum total cost of $263,260, with the algorithm terminating after 22.90 seconds of execution time.

Table 11
Values of binary variables

		s=1	*s=2*	*s=3*	*s=4*	*s=5*	*s=6*
t=1	*m=1*	0	0	1	1	0	0
	m=2	0	0	1	1	0	1
	m=3	0	0	1	0	0	0
t=2	*m=1*	0	0	1	1	0	0
	m=2	0	0	1	1	0	1
	m=3	0	0	1	0	0	0
t=3	*m=1*	0	0	1	0	0	0
	m=2	0	0	1	1	0	0
	m=3	0	0	1	0	0	0
t=4	*m=1*	0	0	1	0	0	0
	m=2	0	0	1	1	0	0
	m=3	0	0	1	0	0	0
t=5	*m=1*	0	0	1	1	0	0
	m=2	0	0	1	1	0	0
	m=3	0	0	1	0	1	0

Table 12
Quantity of AISI 304 steel (kg) supplied by suppliers to manufacturers in all time periods

		s=1	*s=2*	*s=3*	*s=4*	*s=5*	*s=6*
t=1	*m=1*	0	0	3,500	1,000	0	0
	m=2	0	0	2,000	2,500	0	800
	m=3	0	0	3,800	0	0	0
t=2	*m=1*	0	0	3,500	500	0	0
	m=2	0	0	2,000	2,500	0	200
	m=3	0	0	4,350	0	0	0
t=3	*m=1*	0	0	3,250	0	0	0
	m=2	0	0	2,000	2,050	0	0
	m=3	0	0	4,000	0	0	0
t=4	*m=1*	0	0	3,080	0	0	0
	m=2	0	0	2,000	2,050	0	0
	m=3	0	0	4,400	0	0	0
t=5	*m=1*	0	0	3,500	1,600	0	0
	m=2	0	0	700	2,500	0	0
	m=3	0	0	4,500	0	300	0

Table 11 presents the values of the binary decision variables, which indicate whether supplier s is selected by manufacturer m in time period t for the supply of AISI 304 steel used to produce surgical instruments. A value of “1” denotes selection, while “0” indicates otherwise. The supplier selection process was influenced by multiple factors, including the distance between the supplier and manufacturer, the supplier’s maximum capacity and order fulfillment limit, the rejection rate of materials, and the allowable delivery time for each shipment. Table 12 shows the values of continuous variables, representing the amount of AISI 304 steel supplied by selected suppliers to manufacturers in time period “t”.

4.1 Performance evaluation of proposed methodology

To evaluate the performance of the proposed algorithm, the proposed IHGA is compared with other widely used solvers and optimization algorithms. The problem is solved using four alternative approaches: PSO, branch and bound, the interior point method, and a standard genetic algorithm (GA) without fine-tuning. The performance of the IHGA is assessed relative to these methods based on three key criteria: total cost, computational time, and the number of generations required to reach convergence. Table 13 presents the comparative results for all algorithms applied to the same problem instance.

Table 13
Comparison of results of the proposed algorithm with results of other algorithms

Algorithm	Solver package	Performance measures	
		Cost ($)	Computational time (s)
IHGA	MATLAB R2017a	263260	22.91
GA	MATLAB R2017a	266740	61.29
Branch and bound	CPLEX 2016	261370	37.32
Interior point	MATLAB R2017a	259038	43.95
PSO	MATLAB R2017a	275080	18.37

4.2 Comparison of solutions

To compare the results of the algorithms, the solutions must be evaluated relative to the other solutions. Percentage relative gap analysis is performed to assess each performance measure of each algorithm. Imran et al. (2017) used Equation (40) for percentage gap efficiency to compare algorithms. Table 14 provides the basis for drawing conclusions about the relative performance of each algorithm, enabling a comparison across multiple performance metrics. A ranking approach is employed to evaluate and classify the algorithms systematically. Each algorithm is assigned a score on a five-point scale for every performance measure—where a score of five represents the best performance and a score of one represents the poorest. This scoring allows for a comprehensive assessment of overall performance across all criteria. The rankings derived from this evaluation are summarized in Table 18, which presents the comparative performance of each algorithm based on cost, computational time, and number of generations.

$$\%G_{rk} = \frac{AV_{rk} - BV_r}{AV_{rk}} \times 100 \tag{40}$$

Table 14
The percentage gap of each performance measure for each algorithm.

Algorithm	Solver package	Performance measures	
		Cost ($)	Computational time (s)
IHGA	MATLAB R2017a	1.60	0.00
GA	MATLAB R2017a	2.89	62.62
Branch and bound	IBM CPLEX 2016	0.89	38.61
Interior point	MATLAB R2017a	0.00	47.87
PSO	MATLAB R2017a	5.83	13.12

It is evident from Table 18 that the IHGA outperforms all other algorithms, demonstrating superior performance across all evaluated criteria. This enhanced performance is attributed to the optimal balance of cost minimization, reduced computational time, and fewer generations required for convergence. Combining fine-tuning and hybridization in the IHGA leads to more efficient and effective optimization results for the case study problem.

Table 18
Score of each algorithm against all performance measures

Performance measures	Algorithms				
	IHGA	GA	Branch & bound	Interior point	PSO
Cost ($)	3	2	4	5	1
Computational time	5	1	3	2	4
Total score	8	3	7	7	5

4.3 Usefulness of findings

The results obtained in this research are useful for purchasing, marketing, finance, supply chain, and production managers. Flexibility and profitability are two significant benefits of this model.

4.3.1 Flexibility

Traditional multi-period supply chain models are based on current raw materials and transportation prices. Fluctuations in changes in the price of raw materials, transportation, and overhead affect the future costs of a supply chain. Therefore, modeling supply chains with contango and backwardation for predicting future costs would make any supply chain flexible enough to tackle uncertain demands with uncertain changes in supply chain costs caused by uncertain fluctuations in oil prices, raw material prices, and the increasing salaries of employees. Many businesses have failed because of poor resistance to contango and backwardation phenomena around commodities or services in the market. Supply chain planning with contango and backwardation effects provides a high level of flexibility to manufacturers, enabling manufacturers to meet customer demand with the highest profit margin. Future planning in coordination with predicted costs under uncertain changes in the variability of commodities or services must be considered as an essential purchasing decision at a strategic level.

4.3.2 Profitability

Supply chain planning considering contango and backwardation effects has benefits of maintaining or increasing profit margins in each period. Many companies sign contracts with customers around the price of products, and fluctuations in production costs greatly affect companies' profit margins. Companies must consider contango and backwardation effects for all commodities and services involved in their supply chains to maintain or increase profit margins. This research urges supply chain, purchasing, finance, marketing, and production managers to keep an eye on fluctuating prices of commodities and services, affecting overall supply chain costs in upcoming periods. The findings also persuade managers to identify factors that affect the prices of commodities or services over time, as these factors vary across time with the highest levels of uncertainty.

5. Conclusion

This research is conducted in three distinct phases. In the first phase, the contango-backwardation effects are incorporated into a MILP model to minimize total supply chain costs. An integrated polynomial regression fuzzy method is proposed to capture the uncertainty inherent in future cost forecasts. This approach models the forecasted values and the uncertainty associated with those predictions. The second phase introduces a novel IHGA is proposed. In the third phase, a real-world case study involving a group of surgical instrument manufacturers is used to validate the model. Each experiment, as designed through RSM, is executed using the GA. The RSM findings yield optimal parameter settings: a crossover rate of 0.157, a population size 100, and pattern search as the most effective hybrid function. The IHGA, applied with these settings, delivers the best results for the problem set. The IHGA is compared with other algorithms, namely, a standard genetic algorithm (GA), PSO, interior point, and branch and bound, using MATLAB and CPLEX solvers to evaluate its effectiveness. The comparative results confirm that the IHGA outperforms the alternatives regarding computational time, solution cost, and number of generations. The findings of this research emphasize the importance of incorporating contango and backwardation effects in supply chain planning. Models that account for uncertainty and cost fluctuations enhance flexibility and profitability in decision-making. Future research could explore strategic outsourcing decisions in multi-echelon, multi-period, and multi-product supply chain networks, further extending the contango and backwardation modeling scope.

Acknowledgments

This work has been supported by the Basic Scientific Research Project of Wenzhou City, Grant No. G20240020 and G2023036.

Conflict of interest statement

All authors declare they have no conflict of interest or financial conflicts to disclose.

Data availability statement

The data supporting this study's findings are available from the corresponding author, [J.M.], upon reasonable request.

References

Afrouzy, Z. A., Nasseri, S. H., & Mahdavi, I. (2016). A genetic algorithm for supply chain configuration with new product development. *Computers & Industrial Engineering*, *101*, 440-454.

Akbari, A., & Karimi, B. (2015). A new robust optimization approach for integrated multi-echelon, multi-product, multi-period supply chain network design under process uncertainty. *International Journal of Advanced Manufacturing Technology*, *79*.

Awudu, I., & Zhang, J. (2013). Stochastic production planning for a biofuel supply chain under demand and price uncertainties. *Applied energy*, *103*, 189-196.

Benth, F. E., Cartea, Á., & Kiesel, R. (2008). Pricing forward contracts in power markets by the certainty equivalence principle: explaining the sign of the market risk premium. *Journal of Banking & Finance*, *32*(10), 2006-2021.

Changdar, C., Mahapatra, G., & Pal, R. K. (2015). An improved genetic algorithm based approach to solve constrained knapsack problem in fuzzy environment. *Expert Systems with Applications*, *42*(4), 2276-2286.

Čuček, L., Martín, M., Grossmann, I. E., & Kravanja, Z. (2014). Multi-period synthesis of optimally integrated biomass and bioenergy supply network. *Computers & Chemical Engineering*, *66*, 57-70.

Du, Q., Yang, M., Wang, Y., Wang, X., & Dong, Y. (2024). Dynamic simulation for carbon emission reduction effects of the prefabricated building supply chain under environmental policies. *Sustainable Cities and Society*, *100*, 105027.

Fathian, M., Jouzdani, J., Heydari, M., & Makui, A. (2018). Location and transportation planning in supply chains under uncertainty and congestion by using an improved electromagnetism-like algorithm. *Journal of Intelligent Manufacturing*, *29*(7), 1447-1464. https://doi.org/10.1007/s10845-015-1191-9

Garg, H. (2016). A hybrid PSO-GA algorithm for constrained optimization problems. *Applied Mathematics and Computation*, *274*, 292-305.

Imran, M., Kang, C., Lee, Y. H., Jahanzaib, M., & Aziz, H. (2017). Cell formation in a cellular manufacturing system using simulation integrated hybrid genetic algorithm. *Computers & Industrial Engineering*, *105*, 123-135.

Jamrus, T., Chien, C.-F., Gen, M., & Sethanan, K. (2015). Multistage production distribution under uncertain demands with integrated discrete particle swarm optimization and extended priority-based hybrid genetic algorithm. *Fuzzy Optimization and Decision Making*, *14*(3), 265-287.

Lalmazloumian, M., Wong, K. Y., Govindan, K., & Kannan, D. (2016). A robust optimization model for agile and build-to-order supply chain planning under uncertainties. *Annals of Operations Research*, *240*(2), 435-470.

Marzband, M., Azarinejadian, F., Savaghebi, M., & Guerrero, J. M. (2015). An optimal energy management system for islanded microgrids based on multiperiod artificial bee colony combined with Markov chain. *IEEE Systems Journal*.

Meena, P., & Sarmah, S. (2013). Multiple sourcing under supplier failure risk and quantity discount: A genetic algorithm approach. *Transportation Research Part E: Logistics and Transportation Review*, *50*, 84-97.

Miffre, J. (2000). Normal backwardation is normal. *Journal of Futures Markets*, *20*(9), 803-821.

Mousavi, S. M., Alikar, N., Niaki, S. T. A., & Bahreininejad, A. (2015). Optimizing a location allocation-inventory problem in a two-echelon supply chain network: A modified fruit fly optimization algorithm. *Computers & Industrial Engineering*, *87*, 543-560.

Osmani, A., & Zhang, J. (2013). Stochastic optimization of a multi-feedstock lignocellulosic-based bioethanol supply chain under multiple uncertainties. *Energy*, *59*, 157-172.

Özceylan, E., & Paksoy, T. (2013). Fuzzy multi-objective linear programming approach for optimising a closed-loop supply chain network. *International Journal of Production Research*, *51*(8), 2443-2461.

Pasandideh, S. H. R., Niaki, S. T. A., & Asadi, K. (2015). Optimizing a bi-objective multi-product multi-period three echelon supply chain network with warehouse reliability. *Expert Systems with Applications*, *42*(5), 2615-2623.

Ribeiro, D. R., & Hodges, S. D. (2005). A contango-constrained model for storable commodity prices. *Journal of Futures Markets*, *25*(11), 1025-1044.

Rodriguez, M. A., Vecchietti, A. R., Harjunkoski, I., & Grossmann, I. E. (2014). Optimal supply chain design and management over a multi-period horizon under demand uncertainty. Part I: MINLP and MILP models. *Computers & Chemical Engineering*, *62*, 194-210.

Saffar, M., & Razmi, J. (2015). A new multi objective optimization model for designing a green supply chain network under uncertainty. *International Journal of Industrial Engineering Computations*, *6*(1), 15-32.

Soleimani, H., Seyyed-Esfahani, M., & Shirazi, M. A. (2013). Designing and planning a multi-echelon multi-period multi-product closed-loop supply chain utilizing genetic algorithm. *The International Journal of Advanced Manufacturing Technology*, *68*(1-4), 917-931.

Vicente, J. J., Relvas, S., & Barbosa-Póvoa, A. P. (2025). Optimizing inventory planning in multi-echelon supply chains under uncertainty: a decision-making approach using review policies. *International Journal of Management Science and Engineering Management*, 1-17.

Zeballos, L. J., Méndez, C. A., Barbosa-Povoa, A. P., & Novais, A. Q. (2014). Multi-period design and planning of closed-loop supply chains with uncertain supply and demand. *Computers & Chemical Engineering*, *66*, 151-164.